Supporting Online Material for

Amazon Forests Green-Up During 2005 Drought

Scott R. Saleska,* Kamel Didan, Alfredo R. Huete, Humberto R. da Rocha

*To whom correspondence should be addressed. E-mail: saleska@email.arizona.edu

This PDF file includes:

Materials and Methods
Figs. S1 to S3
References

Supporting Online Material

Brevia: Amazon Forests Green-up during 2005 drought

Scott R. Saleska, Kamel Didan, Alfredo R. Huete, and Humberto R. da Rocha

Materials and Methods

Rainfall data are from the TRMM (Tropical Rainfall Measuring Mission, 3B43-v6) satellite timeseries (1998-2006), at 0.25° x 0.25° resolution (*S1*), which we super-sampled to interpolate onto a higher resolution (1 km) grid and match the resolution of greenness data (see below). The TRMM 3B43-v6 dataset is derived by combining basic TRMM data with the infrared-based Geostationary Operational Environmental Satellite Precipitation Index (GOES-PI) and with a global network of gauge data (*S2*). Regional validation studies, e.g. in tropical West Africa (*S3*) and in the Brazilian Amazon (*S4*), show strong agreement at monthly timescales between the blended TRMM product and independent ground based rain gauge data, except for wet months (rainfall > 300 mm month^{-1}) due to underestimation of high rainfall events (*S4*).

Soil moisture is more relevant than precipitation for vegetation, but is sparsely observed in the Amazon. For the purposes of this study, however, it is sufficient if precipitation variation is a good proxy of soil moisture variation. Comparisons at a site in the central Amazon in fact show (Fig. S1) rapid response of soil moisture to precipitation changes at the 2-3 m depths typically used in major vegetation model studies (e.g., Hadley Center's TRIFFID model, *S5,* or the IBIS model, *S6*). This correlation between precipitation and soil moisture maximizes at a lag of l month (Fig. S1), consistent with the prompt (~1 month lag) drought-induced reduction in forest photosynthesis seen in these models (*S5*). The prompt modeled response to drought implies that the 2005

drought, at 3-4 months duration, should be more than long enough to reveal this modeled

vegetation dynamic, if it exists, and that our comparison of precipitation and vegetation

anomalies, based on quarterly aggregation (see below), should detect it.

Canopy greenness is represented by the Enhanced Vegetation Index (EVI),

composited each 16 days from the Moderate Resolution Imaging Spectroradiometer

(MODIS) on the Terra satellite (*S7*). MODIS-detected surface reflectances are corrected

for atmospheric distortion from ozone and aerosols, relying on narrow spectral bands to

minimize water vapor influences (*S7*). We used high-resolution (1 km) data to facilitate

removal of cloud and shadow-contaminated pixels from the image (*S8*). Our cloud-

filtered MODIS EVI correctly detects opposite seasonal patterns of gross ecosystem

productivity (GEP) in adjacent pasture and forest sites (as measured by ground-based flux

towers), even in the face of similar seasonal patterns in potential sources of

contamination (clouds and aerosols) across sites (*S8*). From this we infer that our

reported EVI patterns are unlikely to be the result of atmospheric artifacts.

Within each pixel, anomalies in precipitation and canopy greenness for 2005 were

calculated for each quarter, *q*, as the departure from the longer-term mean for that

quarter, $\bar{x}_q$, normalized by the standard deviation around that quarter's longer-term mean,

across years (σ_q):

$$ANOMALY_{2005,q} = \frac{x_{2005,q} - \bar{x}_q}{\sigma_q} \qquad (1)$$

where $x_{2005,q}$ is the data value for quarter q – the cumulative (for precipitation) or average

(for EVI) of all data within the quarter – and $\bar{x}_q$ and σ_q are calculated across the years of

data availability (1998-2006 for TRMM precipitation, 2000-2006 for MODIS EVI, with

2005 excluded). We report results here for the Jul – Sept. quarter, which experienced the most intense drought (*S4*), and which also showed the strongest EVI response.

Considering only EVI anomalies observed within the TRMM precipitation-defined drought area (Fig S2), we quantified the statistical significance of the observed EVI anomaly distribution (Fig 1C, in which 64% of anomalies are positive) by comparison to the binomial distribution under the null hypothesis that independent forest patches are equally likely to exhibit positive or negative EVI anomalies. The scale at which different patches of forest "greenness" can be treated as independent presumably corresponds to the scale of individual hydrological catchments -- likely larger than a MODIS pixel (1 km x 1 km), but almost certainly smaller than a 1° x 1° square (110 km on a side). Conservatively assuming that independence is achieved only as patch area approaches 1° x 1°, we note that the TRMM precipitation-defined drought area (Fig S2) occupies 2.2 million km^2, or approximately ~ 180 1° x 1° squares; the binomial probability of observing at least 64% positive anomalies out of 180 under the null hypothesis is very low (*p < 0.0001*).

Areas outside the Amazon region (as defined in *S9*) were not included in our analysis. Areas with land-cover dominated by human activities or by non-forest vegetation (areas like those in (a) and (b) of Fig. S3) were excluded from the EVI anomaly distribution reported in Fig 1C.

Fig S1. **(A)** Monthly precipitation observed from TRMM satellite (*S1*) and from ground-based tower gauge (*S10*), and **(B)** soil moisture measured by frequency-domain reflectometry at the same location as the rain gauge (*S10*), at the km 83 site in the Tapajós National forest in the central eastern Amazon (3.01030° S, 54.58150° W). Linear regression of TRMM vs. rain gage precipitation in (A) gives a slope of 1.03 ($R^2 = 0.72$). The correlation between local precipitation (A), and local soil moisture (B), averaged over the top 3m, maximizes at 1 month lag (with $R^2 = 0.61$).
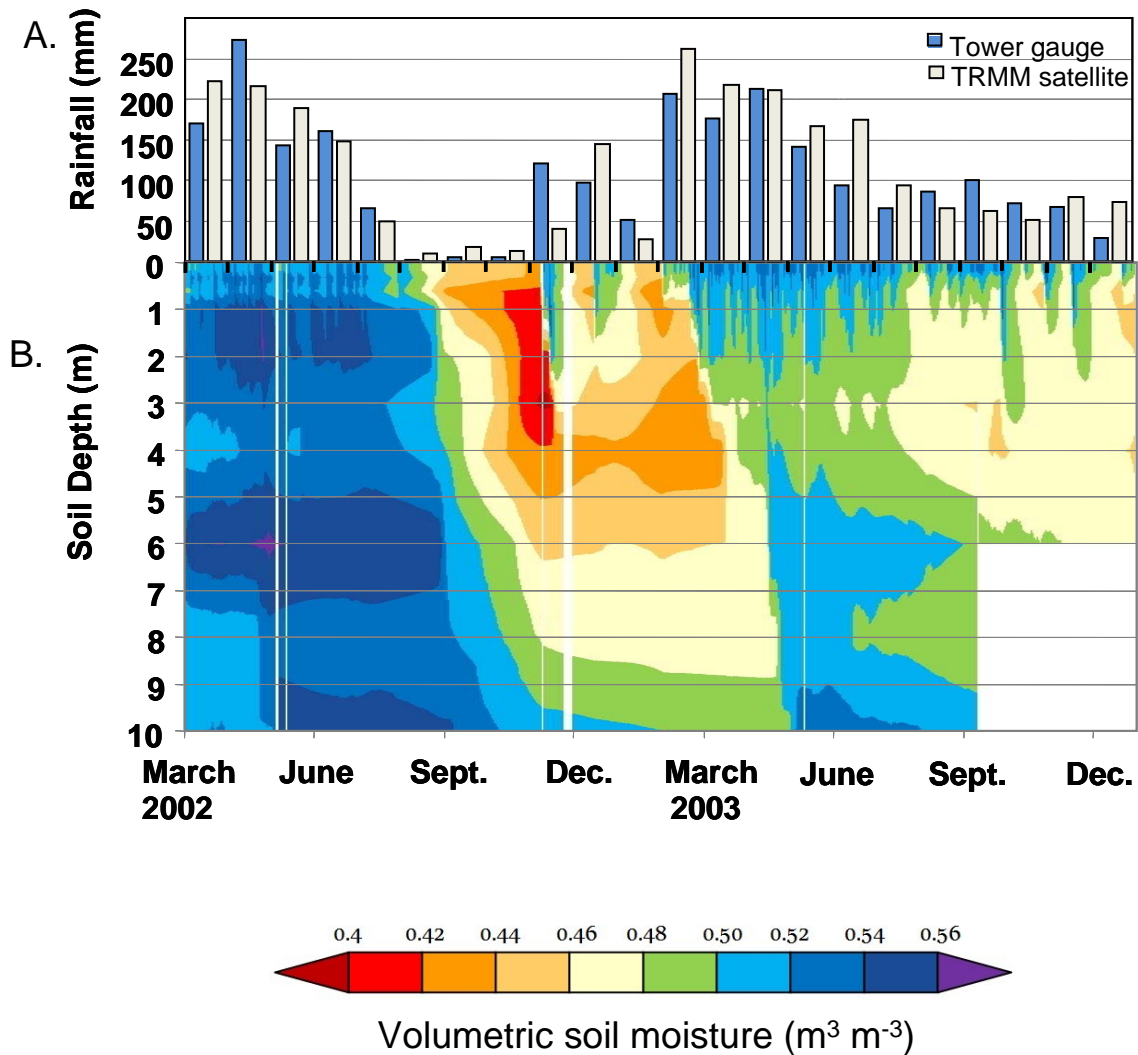
Fig S2. Intact forest EVI anomalies from Fig. 1B that are also within the drought area defined by red pixels in Fig 1A (those pixels in which the quarterly precipitation was more than one standard deviation below the mean). EVI anomalies not in this drought area, or in areas dominated by human activity or non-forest vegetation (Fig S3), are masked by gray and excluded from the anomaly distribution depicted in Fig 1C.
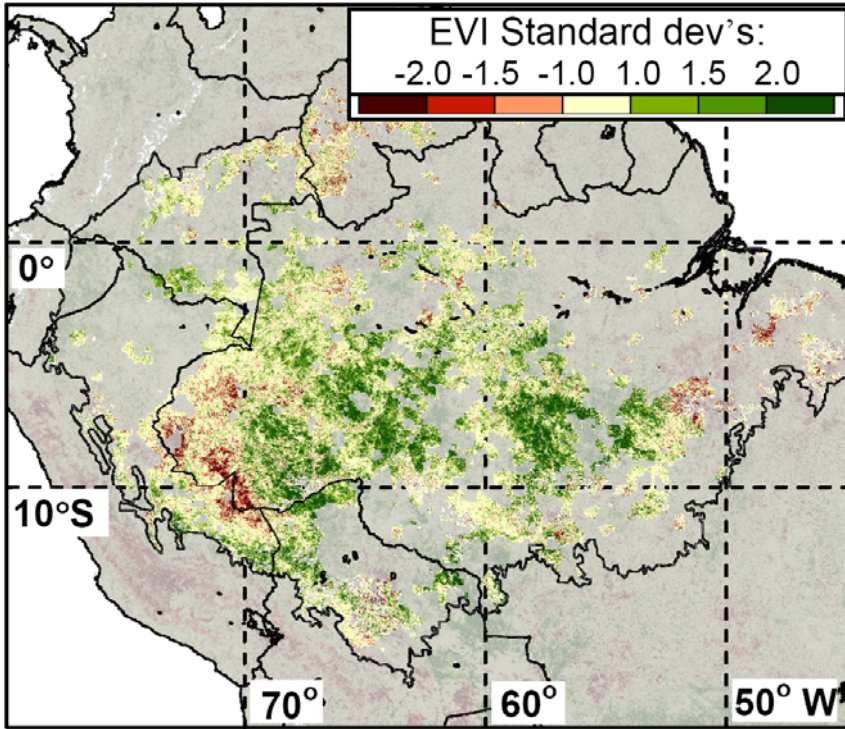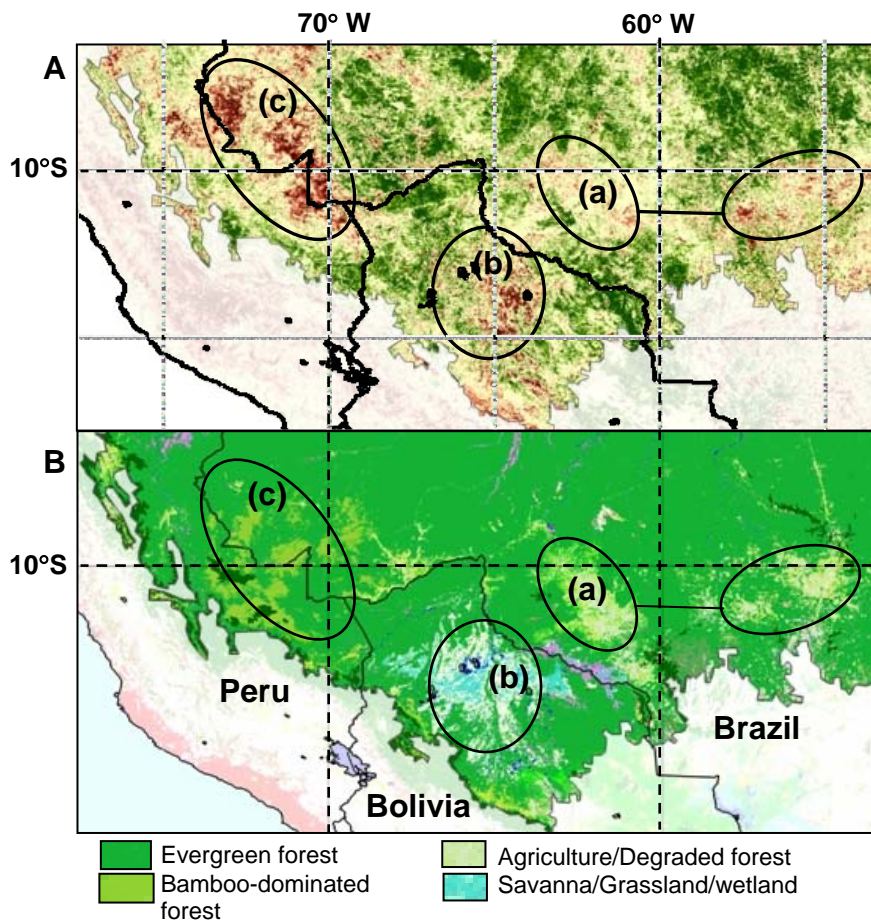
Fig S3. **(A)** Close-up of EVI anomalies from Fig. 1B, and **(B)** corresponding land-cover types as of 2000 (*S11*). Highlighted areas, with no increase or a decline in MODIS EVI, include: (a) deforested/converted areas in the Brazilian states of Rondônia (left oval) and Mato Grosso (right oval), (b) the Beni Savanna/wetland, in the lowlands of northern Bolivia, a non-forest biome (*S12*), and (c) Bamboo-dominated or Bamboo-susceptible forests along the border between Peru and the Brazilian state of Acre. Amazon forests dominated by Bamboo are rare (found nearly exclusively in the area depicted here), with low rates of tree recruitment and low biomass (*S13*). Bamboo are thought to take hold in regions where dense soil horizons block tree taproot penetration, and hence, they are a possible indicator of forests with relatively limited access to deep soil water (*S14*).

 Supporting Material References

S1. NASA (2007), 3B43: Monthly 0.25° × 0.25° TRMM and other sources rainfall, http://disc.sci.gsfc.nasa.gov/services/opendap/trmm.shtml, NASA Distrib. Active Arch. Cent., Goddard Space Flight Cent. Earth Sci., Greenbelt, Md.

S2. R.F. Adler, A.J. Negri, D.T. Bolvin, S. Curtis, E.J. Nelkin, *J. Appl. Meteor.* **39**, 2007-2023 (2000).

S3. S.E. Nicholson, *et al.*, *J. Appl. Meteor.* **42**, 1355-1368 (2003).

S4. L.E.O.C. Aragão, Y. Malhi, R.M. Roman-Cuesta, S. Saatchi, Y.E. Shimabukuro, *Geophys. Res. Lett.* **34**, L07701 (2007).

S5. C.D. Jones, *et al.*, *J. Climate* 14, 4113-4129 (2001).

S6. M.H. Costa, J.A. Foley, *J. Geophys. Res.* **102**, 23973-23989 (1997).

S7. C.O. Justice, J.R.G. Townshend, E.F. Vermote, E. Masuoka, R.E. Wolfe, *et al.*, *Rem. Sens. Env.* **83**, 3-15 (2002).

S8. A.R. Huete, K. Didan, Y.E. Shimabukuro, P. Ratana, S.R. Saleska, L.R. Hutyra, W. Yang, RR. Nemani, R. Myneni, *Geophys Res. Lett.*, **43**, L06405 (2006).

S9. H. D. Eva, O. Huber (Eds.), "A proposal for defining the geographical boundaries of Amazonia," (Rep. EUR 21808-EN, Off. Publ. Eur. Communities, Luxembourg, 2005).

S10.   R.D. Bruno, H.R. Rocha, H.C. Freitas, M.L. Goulden, S.D. Miller, *Hydrol. Processes* **20**, 2477-2489 (2006).

S11.   H.D. Eva, A.S. Belward, E.E. De Miranda, C.M. Di Bella, V. Gond, *et al. Glob. Change. Biol.* **10**, 731-744 (2004). Land-cover map data available at: http://www-gem.jrc.it/glc2000/Products/southamer/Maps/Thematic/sam_thematic1A.htm.

S12.   R. Haase, S.G.Beck, *Brittonia*, **41**, 80-100 (1989).

S13.   B.W. Nelson, A.C.A. Oliveira, G.T. Batista, D. Vidalene, M. Silveira, in *Proc. 10th Brazilian Remote Sensing Symposium*, Foz de Iguacu, Paraná, Brazil, INPE (2001).

S14.   B.W. Griscom, P.M.S. Ashton, *For. Ecol. Man.* **175**, 445-454 (2003).